Earthquake Engineering, Tenth World Conference © 1992 Balkema, Rotterdam. ISBN 90 5410 060 5

Prediction of site-specific strong ground motion using semi-empirical methods

Katsuhiro Kamae
Research Reactor Institute, Kyoto University, Japan

Kojiro Irikura
Disaster Prevention Research Institute, Kyoto University, Japan

ABSTRACT: We propose two methods for estimating input motion at a objective site for earthquake resistant design of a structure. One is the so-called empirical Green's function method. Its essence is to construct a large earthquake by a superposition of many small-ones based on the regional scaling relation of source parameters estimated from earthquakes occurring in the objective region, and to correct the small-event motions to be appropriate Green's functions by considering the differences in stress drop, attenuation effects due to propagation media, high-frequency cutoff (f_{max}) of acceleration spectra, and radiation patterns between large and small events.

Although this method is useful in cases where appropriate observation records exist for empirical Green's functions, in practical prediction problems, these are not always available. Therefore, we present the other synthesis method using stochastically simulated small-event motions based on a seismological spectral model and making delay-sum of small events in the same manner as empirical Green's function method. Finally, we attempt to predict strong ground motion due to a future large earthquake (M=7, Δ=13km) by means of the two methods. We find that the characteristics of both synthetic motions are in good agreement with each other, and comparable to the empirical value in the maximum peak acceleration. As a result, the latter method can also be applied to the prediction of strong ground motion as long as small-event motions are simulated to follow the ω^{-2} spectral scaling law and to include the propagation path effects.

1 INTRODUCTION

It is desirable that the input motion for the earthquake resistant design of a structure is estimated in consideration of source, path and local site effects. In simulating such motion for purposes of engineering design, the empirical Green's function method is one of the most effective techniques. This method not only has the advantage of including propagation path effects and local site effects, but also is capable of incorporating the effects of rupture propagation on the fault plane and geometrical relation between source and station.

In this paper, we present two synthesis methods for predicting strong ground motion at a specific site from a future large earthquake. One is the case of using observed motions as empirical Green's functions, and the other is using stochastically simulated motions as semi-empirical Green's functions. Although the empirical Green's function method is the best, we can not always find any appropriate records in the objective region. We need to develop a complementary method for such a case. Although the latter lacks the advantage of incorporating the propagation path effects and local site effects, we can give these effects from the empirical relation of attenuation factors in the objective region and numerical estimation of site responses based on geologic structure. Finally, we attempt to predict the strong ground motions due to a future large earthquake (M=7,Δ=13km) by means of the two methods. Comparing the results obtained by the two methods, we examine the validity of applying the latter method to the prediction of strong ground motion.

2 REGIONAL SCALING RELATION OF SOURCE PARAMETERS

We construct the ground motion from a large earthquake by superposition of those from small events occurring near the source area of the large earthquake. Therefore, it is very important for synthesis to estimate regional scaling relations of source parameters based on the observed data in the objective region. In this paper, we use the data of six earthquakes with magnitudes ranging between 4.4 and 5.6 which occurred in the objective region (*Kinki* district, *Japan*). We determined the next regional relationship between seismic moment M_0 and the corner frequency f_c by least squared method.

$$\log M_0 = -3.0 \log f_c + 23.1 \qquad (1)$$

Replacing f_c by the fault area S using *Sato and Hirasawa's* formula, we have following equation.

$$\log M_0 = 1.5 \log S + 23.08 \qquad (2)$$

3 SYNTHESIS METHOD

We use the following synthesis formulation proposed by Irikura (1986), which is effective in the case that both large and small events have ω^{-2} spectral characteristics.

$$U(t) = \sum_{i=1}^{N} \sum_{j=1}^{N} \frac{r}{r_{ij}} F(t - t_{ij}) * u_{ij}(t) \qquad (3)$$

where

$$t_{ij} = \frac{(r_{ij} - r_0)}{V_s} + \frac{\xi_{ij}}{V_R} \quad ,$$

$$F(t) = \delta(t) + \frac{1}{n'} \sum_{k=1}^{(N-1)n'} \delta\left[t - (k-1)\frac{\tau}{(N-1)n'}\right] \quad ,$$

$U(t)$ and $u_{ij}(t)$ are synthetic motion for large earthquake and Green's function appropriate for each sub-fault, respectively. The parameter N is determined from the cubic root of the seismic moment ratio between large and small events. Then, the ratio of source area between both events should be N^2 and the ratio of rise time should be N as long as the scaling relations are ideally applicable based on constant stress drop. r, r_{ij}, and r_0 are distances from the site to the hypocenter of a small event, from the site to the (i,j) sub-fault and from the site to the starting point on the fault plane of the large event, respectively. ξ_{ij} is the distance between the starting point and the (i,j) sub-fault. V_s is the shear wave velocity, V_R is the rupture velocity, n' is arbitrary number, and τ is the rise time of the large event.

3.1 Empirical Green's function method

In order to obtain Green's function appropriate for each subfault, the small-event motion $u_0(f)$ is needed to correct in the frequency domain as shown in equation (4) by considering the differences in stress drop, radiation patterns, high-frequency cutoff (f_{max}) of acceleration spectra, and attenuation effect due to propagation media between large and small events.

$$u_{ij}(f) = \alpha \frac{R_{ij}(\theta,\phi)}{R(\theta,\phi)} F(f, f_{max}) \, e^{\pi f \left(\frac{r - r_{ij}}{Q_s(f)\, V_s}\right)} \, u_0(f) \qquad (4)$$

where α is stress drop ratio of large earthquake to small one. $R_{ij}(\theta,\phi)$, $R(\theta,\phi)$ are radiation coefficients for the (i,j) sub-fault and small-event, respectively. $F(f,f_{max})$ is high-cut filter to correct the difference of the f_{max} between large and small events, and is given as

$$F(f, f_{max}) = \frac{1 + \left(\frac{f}{f^s_{max}}\right)^n}{1 + \left(\frac{f}{f^m_{max}}\right)^n} \qquad (5)$$

where the superscripts m and s indicate the values for large and small events. f_{max} is given from the empirical dependence of the f_{max} on seismic moment M_0 obtained by Faccioli (1986) as shown by

$$f_{max} = 7.31 \times 10^3 \, M_0^{-0.12} \qquad (6)$$

$Q_s(f)$ is frequency-dependent Q-value for shear wave. We use $Q_s(f) = 110\sqrt{f}$, which is the empirical relation in the *Kinki* district, *Japan* obtained by Akamatsu, 1980.

Now, we describe the correction procedure for radiation patterns, that is, how to obtain the above $R_{ij}(\theta,\phi)$ and $R(\theta,\phi)$. Even if both the source mechanisms of the large and the small events are similar, the contribution of the radiation characteristics from each subfault to the site remarkably varies depending on the subfault location on the large fault plane, especially in the case of a site near to a large fault. The radiation patterns are evaluated independently of frequency from the theory of a point source radiation. However, according to Liu and Helmberger (1985), observed ground motions show little agreement to theoretical ones at high frequencies (>5Hz) because of scattering effects due to heterogeneous propagation media, although they seem to converge with theoretical ones at low frequencies (<0.5Hz). In order to describe such empirical frequency-dependent radiation patterns, we propose the following technique.

Boore et al. (1984) calculated the average radiation coefficients by the following integral

$$\langle G \rangle = \frac{\int_0^{\pi}\int_0^{2\pi} [W(\theta,\phi) G(\theta,\phi)] \sin\theta \, d\phi d\theta}{\int_0^{\pi}\int_0^{2\pi} [W(\theta,\phi)] \sin\theta \, d\phi d\theta} \qquad (7)$$

where G is taken to be F^2, $|F|$, or $\log|F|$, and F is

the radiation pattern for the appropriate type of wave. Φ is the azimuth and θ is the take-off angle. They assumed that the weighting function $W(\theta,\phi)$ is independent of azimuth and is nonzero (and equal to one) only for take-off angles in the range $\theta_1<\theta<\theta_2$

$$W(\theta,\phi)=H(\theta-\theta_1)-H(\theta-\theta_2) \qquad (8)$$

where $H(\theta)$ is the Heviside step function. We also use equation (7) under the weighting function defined by

$$W(\theta,\phi)=(H(\theta-\theta_1)-H(\theta-\theta_2))\cdot (H(\phi-\phi_1)-H(\phi-\phi_2)) \qquad (9)$$

which is nonzero (and equal to one) only for take-off angles θ in the range $\theta_1<\theta<\theta_2$ and azimuth ϕ in the range $\phi_1<\phi<\phi_2$. Consequently, we can evaluate the frequency-dependent radiation pattern $G(\theta,\phi,f)$ under the assumption that the range of ϕ, i.e., $\Delta\phi$ shown in Fig.1 is represented by a function of frequency as shown in Fig.2. The range of θ is frequency-independent and focal distance-dependent as described by Boore et al. (1984). The smoothed radiation coefficients are taken to have the same signs as the theoretical ones.

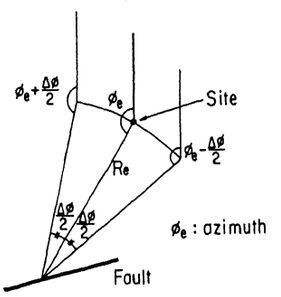

Fig.1 The geometry of azimuthal range $\Delta\phi$, for averaging radiation coefficient.

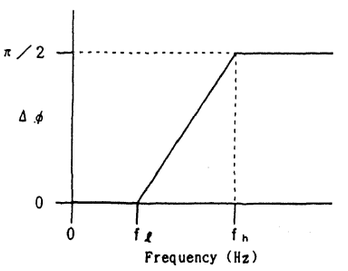

Fig.2 The assumed frequency-dependence of $\Delta\phi$, where f_ℓ and f_h are given to be 0.5 Hz and 5 Hz.

Now we will examine the frequency-dependent radiation pattern in the case of the strike-slip type on a vertical fault to check the above method numerically. Fig.3 shows each radiation pattern in <0.5Hz, 2Hz, 3Hz, 4Hz, and >5Hz. We can see that the higher the frequency is, the smoother the radiation pattern. Furthermore, in order to evaluate the radiation pattern $G(\theta,\phi)$ in equation (7), we need to determine the strike, the dip angle and the rake angle of the fault. Therefore, when it is difficult to uniquely estimate these parameters, we must examine the parametric variation of synthetic results in applying this correction to low-frequency ground motion prediction.

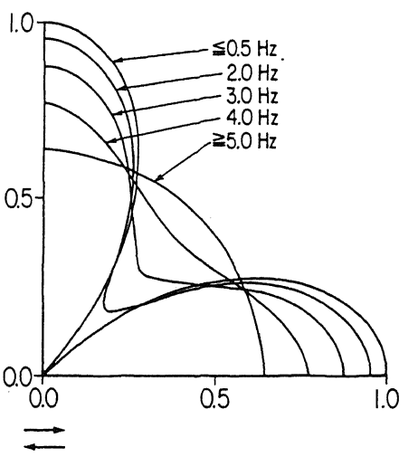

Fig.3 The frequency-dependent radiation pattern of transverse component in case of the strike slip type on a vertical fault.

3.2 Revised stochastic simulation method

We stochastically simulate the small-event motions as semi-empirical Green's functions in cases where no suitable records of actual small-events are available. Boore (1983) proposed a simple method to simulate high-frequency ground motions based on a seismological spectral model. His idea is to generate a stochastic time series of filtered and windowed Gaussian white noise whose acceleration amplitude spectrum is matched, on the average, to an ω-squared spectrum with a high-frequency cutoff (f_{max}). Although he considers the seismological spectral model, the physical characteristics of seismic source, such as fault size, slip and rupture propagation, are not taken into account. The strong ground motions near to a large earthquake are severly influenced by the spacial extent of slip and rupture propagation on the fault

plane. Therefore, *Boore's* method may not be available for estimating near-field motions.

We use his method only for simulating the motion from a small-event because of its small size and the effect of rupture propagation is negligible. The specified acceleration spectrum $A(f)$ of shear waves at a distance X from a fault with seismic moment M_0 is

$$A(f)=CM_0S(f, f_c)P(f, f_{max}) \frac{e^{\frac{-\pi fX}{Q_s(f)V_s}}}{X} \qquad (10)$$

where

$$C=\frac{R(\theta,\phi)\cdot FS\cdot PRTITN}{4\pi\rho V_s^3} \quad ,$$

$R(\theta,\phi)$is the radiation pattern, FS is the amplification due to the free surface, $PRTITN$ is the reduction factor that accounts for the partitioning of energy into two horizontal components, and ρ is the density. The source spectrum S is given by equation (11). The high-cut filter P is assumed to be equation (12) in the present paper.

$$S(f, f_c)=\frac{(2\pi f)^2}{1+(\frac{f}{f_c})^2} \qquad (11)$$

$$P(f, f_{max})=\frac{1}{1+(\frac{f}{f_{max}})^n} \qquad (12)$$

where f_c is corner frequency. n equals to 1. As we have seen, using equations (1) and (6), the spectrum $A(f)$ can be specified by only one parameter : seismic moment M_0.

Next, we use a shaping window whose length is controlled by the following empirical relation between duration time (T_D) and magnitude (M) obtained by Hisada and Ando (1976) because our observation results are also satisfied by the relation.

$$\log T_D=0.31\ M - 0.77 \qquad (13)$$

The other parameters needed in the simulation were taken to be : ρ=2.7 g/cm^3, V_s=3.6 km/sec, $R(\theta,\phi)$=0.63, Qs=$110\sqrt{f}$ (used in the preceding chapter), $PRTITN$=0.71, and FS=2 (in this paper, simulated small-event motion is defined on the outcropping rock).

We can generate many simulated ground motions by simply changing the seed of the pseudo-random number generator. For semi-empirical Green's function, we use the appropriate one from among simulated motions by checking if Fourier amplitude spectra are in reasonable agreement with the desired spectrum. The synthesis computation is carried out in the same manner as empirical Green's function method.

4 SYNTHESIS OF LARGE EARTHQUAKE OF M7

We attempt to synthesize the strong ground motion from a future large earthquake by means of the two methods described above. One is using actual small-event motion and the other is using stochastically simulated small-event motion. The target is the large earthquake with magnitude 7 caused by the *NEGORO* active fault in *Wakayama, Japan*. The epicenter of the actual small-event (M=4.4) used as empirical Green's function is shown in Fig.4 by the symbol (★) together with the location of the fault and the observation site. On the other hand, we used a stochastically simulated small-event motion from an earthquake with magnitude 5 at a distance of 20 km as a semi-empirical Green's function. The source parameters of the target event, those of the actual small-event and the stochastically simulated event are summarized in Table 1 and Table 2, respectively. The fault dimensions and the geometry are determined by a reference. The seismic moment of the target event is estimated from the regional scaling relation (equ. (2)).

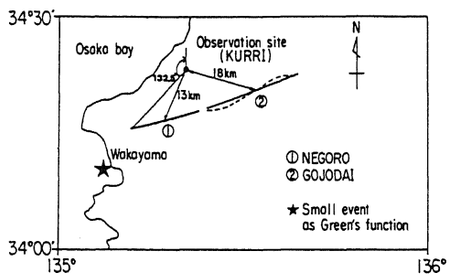

Fig.4 Locations of observation site, the *NEGORO* fault and actual small-event

Table 1. Source parameters for the target earthquake.

Strike	N74°E
Dip	90°
Slip type	right strike slip
Length	20 km
Width	10 km
Seismic moment	3.4×10^{26} dyne·cm
Rise time	1.6 sec
Stress drop	293 bar
Rupture velocity	2.5 km/sec
Shear wave velocity	3.6 km/sec

Table 2. Source parameters for the small earthquakes.

M	X (km)	M_0 (dyne·cm)	S (km^2)	σ_R
4.4	32	2.97×10^{22}	0.43	1.1
5	20	3.40×10^{23}	2.0	1.0

σ_R : The ratio of large event's stress drop to small event's

The synthetic acceleration motions of the horizontal component ($E-W$) in the objective site are shown in Fig.5, together with the small-event motions as Green's functions. Both synthetic motions are bandpass filtered between 0.5 Hz and 20 Hz by considering the reliable frequency range of the actual small-event motion. Each resultant motion is synthesized under the condition that rupture starts at mid-point of the fault bottom and extends radially. Peak accelerations , peak velocities and duration times (calculated from Trifunac and Brady, 1975) of the synthetic motions are summarized in Table 3. The synthetic velocity response spectra are shown in Fig.6.

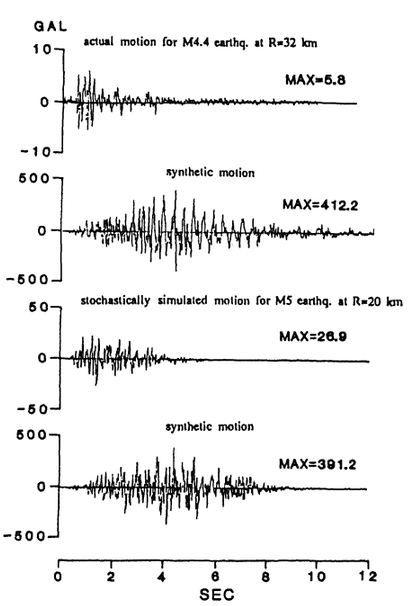

Fig.5. Small-event motions and synthetic motions. Upper two figures show actual motion and synthetic motion using that. Lower two figures show stochastically simulated motion and synthetic motion using that.

Table 3. Peak accelerations, peak velocities and duration times of the synthetic motions.

Small event	Maximum peak		Duration time
(magnitude)	Acc. (gal)	Vel. (kine)	(sec)
4.4	412.2	21.5	5.7
5	391.2	17.7	4.9
empirical	405.6	—	—

empirical : The value calculated from Equation (14)

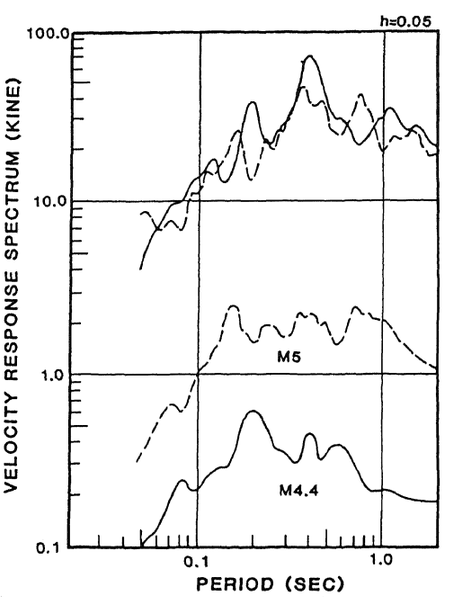

Fig.6 Velocity response spectra for synthetic motions. Solid line and broken line are spectra for synthetic motions using actual motion and stochastically simulated one, respectively.

5 DISCUSSION

In Fig.5, both synthetic waveform envelopes are similar to each other. We find that both peak accelerations are similar to each other and comparable to the value estimated from the following empirical formula obtained by Fukushima and Tanaka (1990).

$$\log A = 0.41M - \log(R+0.032\cdot10^{0.41M}) - 0.0034R + 1.30 \quad (14)$$

where A is the peak acceleration, R the shortest distance between site and fault rupture (=10 km), and M the magnitude (=7). The duration time of synthetic motion

using the stochastically simulated one tends to be slightly shorter than that obtained when using actual motion. This discrepancy may be caused by different definitions of the duration times. It is apparent from Fig.6 that both spectral amplitudes are in the same range in the natural period range of 0.05 to 2 seconds, although predominant periods are not in detailed agreement with each other. The reason for discrepancies of the predominant periods may be attributed to taking no account of the local site effects when simulating the small-event motions as semi-empirical Green's functions.

From these results, we can conclude that the present empirical Green's function method is very powerful when predicting the strong ground motion for a future large earthquake, and that it should be possible to use the stochastically simulated small-event motion as semi-empirical Green's function in cases where no appropriate observation records are available.

CONCLUSIONS

Two semi-empirical methods have been proposed to predict strong ground motions due to a future large earthquake. One is the empirical Green's function method. The synthesis was performed by considering the differences in stress drop, attenuation effects due to propagation media, high-frequency cutoff (f_{max}) of acceleration spectra, and radiation patterns between large and small events. The other is a revised stochastic simulation method employed when no suitable observation data as empirical Green's functions. In this method, we used the stochastically simulated small-event motion based on seismological spectral model as semi-empirical Green's function, instead of the actual motions. Finally, we have tried to predict the strong ground motions due to a future large earthquake (M=7,Δ=13km) by means of the two methods.

From these results, we can conclude that (1) the empirical Green's function method proposed in this paper is powerful enough to estimate such motions for purposes of engineering design, and that (2) in case of having no appropriate observation records of the objective site, it should be possible to use the small-event motions simulated in this paper as substitute for the actual motions.

REFERENCES

Akamatsu, J. 1980. Attenuation property of seismic waves and source characteristics of small earthquake. *Bull. Disas. Prev. Inst.,Kyoto Univ.* Vol.30 :53-80.

Boore, D.M. 1983. Stochastic simulation of high-frequency ground motions based on seismological models of the radiated spectra. *Bull. Seism. Soc. Am.* Vol.73 No.6 :1865-1894.

Boore, D.M. and J. Boatwright 1984. Average body-wave radiation coefficients. *Bull. Seism. Soc. Am.* Vol.74 No.5 :1615-1621.

Faccioli, Ezio. 1986. A study of strong motions from Italy and Yugoslavia in terms of gross source properties. *Geophys. Monograph* 37 *Maurice Ewing* 6 :297-309.

Fukushima, Y. and T. Tanaka 1990. A new attenuation relation for peak horizontal acceleration of strong earthquake ground motion in japan. *Bull. Seism. Soc. Am.* Vol.80 No.4 :757-783.

Hisada, T. and H. Ando 1976. Relation between duration of earthquake ground motion and the magnitude. *Kajima Institute of Construction Technology Report.*

Irikura, K. 1986. Prediction of strong acceleration motion using empirical Green's function. *Proc. 7th Japan Earthq. Eng. Symp.*:151-156.

Liu, H.L. and D.V. Helmberger 1985. The 23:19 aftershock of the 15 october 1979 imperial valley earthquake: more evidence for an asperity. *Bull. Seism. Soc. Am.* Vol.75 No.3 :689-708.

Sato, T. and T. Hirasawa 1973. Body wave spectra from propagating shear cracks. *J. Phys. Earth.* Vol.21:415-431.

The Research Group for Active Faults 1991. *Active faults in Japan -sheet maps and inventories-* :280-285. (*in Japanese*)

Trifunac, M.D. and A.G. Brady 1975. A study on the duration of strong earthquake ground motion. *Bull. Seism. Soc. Am.* Vol.65 :581-626.